P. S. Damerell[1]
MPR Associates, Inc.
Washington, D. C.

R. J. Schoenhals
Professor of
Mechanical Engineering,
Purdue University,
West Lafayette, Ind.,
Mem. ASME

Flow in a Toroidal Thermosyphon with Angular Displacement of Heated and Cooled Sections

A toroidal thermosyphon consisting of a fluid-filled torus located in a vertical plane was studied analytically and experimentally. Good agreement was obtained between analytical predictions and measurements for large values of the angular displacement of the heated and cooled sections. For smaller angular displacements, the analytical predictions of steady state flow rates were found to exceed the corresponding experimentally observed values. The discrepancies were attributed to a reverse flow phenomenon. Some analytically predicted flows were not physically achievable. In these situations the flow would either reach a steady condition in the opposite direction, or it would oscillate indefinitely.

Introduction

This paper is concerned with the buoyancy-driven flow of a single phase fluid inside a torus located in a vertical plane. Such a device is referred to as a toroidal thermosyphon (Fig. 1). Various types of thermosyphons are used for cooling purposes in industrial processes. A major advantage of these devices is that efficient heat removal is achieved by a flowing fluid without the need for a pump. Flow in a toroidal thermosyphon is driven by buoyancy forces created by heating and cooling of the internal fluid. The motion of the fluid is opposed by frictional shear forces between the fluid and the wall of the torus. For fixed heat addition and heat removal conditions, the steady-state flow rate in the thermosyphon is the value for which buoyancy and frictional forces are balanced. The circulatory flow is enhanced by larger heat addition rates because the fluid density differences within the thermosyphon are increased. Also, as the heat addition section is moved toward the bottom of the thermosyphon and the heat removal section toward the top, the flow rate increases. This behavior is contrary to the concept that a closed loop thermosyphon should be heated and cooled along its sides, with the fluid rising through the heated side and falling through the cooled side, as suggested by some other investigators of the problem [2–4]. The determination of flow rate when the heat source is at the bottom and the heat sink at the top is shown in [5–7].

The purpose of the present study was to investigate the variation in steady flow rate with angular displacement of the heated and cooled sections for a thermosyphon of simple well-defined geometry. A toroidal geometry heated over one-half its area and cooled over the remaining half was selected. Straightforward, one-dimensional models were developed to predict the variation of flow rate with angular displacement and these predictions were compared with experimental results. The effects of fluid properties, system dimensions and heat transfer rate on flow rate have been thoroughly discussed in previous literature [5–8] and were not specifically investigated in this study.

It has been shown analytically [5–7] and confirmed experimentally [5] that steady flow is not achievable in a closed loop thermosyphon for a certain range of heat input. In these cases unstable flow occurs and the flow rate oscillates with increasing amplitude until it eventually reverses direction, whereupon oscillations initiate in the new flow direction. Prediction and observation of this behavior have been previously performed only for a thermosyphon which was heated from directly below and cooled from directly above. At the outset of this investigation it was expected that this unstable flow behavior would also occur when the positions of the heated and cooled sections were altered. Results from an experimental study of this topic are also included in this paper.

Analysis

The analysis which follows predicts the steady flow velocity for a toroidal thermosyphon which is heated continuously over one-half its area and cooled continuously over the remaining half. Some portions of the analysis are condensed for conciseness. Complete details are contained in [1]. Although both steady and unsteady flow were encountered in the experimental portion of this work, only a steady flow analysis is presented herein. An analysis which predicts unsteady flow conditions is presented in [5]. The thermosyphon considered in the analysis is shown in Fig. 1. The analysis assumes steady laminar flow, and assumes the Boussinesq approximation is valid. Density is assumed to be a linear function of temperature, which varies only with θ. Axial conduction and viscous dissipation are neglected and viscosity, specific heat and thermal conductivity are assumed to be constant. Also, the effect of curvature on the flow is neglected. An investigation of the validity of this assumption carried out utilizing [9] showed that the effect of curvature would be expected to influence the prediction of flow rate by only ten to fifteen percent for the thermosyphon considered in the experimental portion of this study. Using an incre-

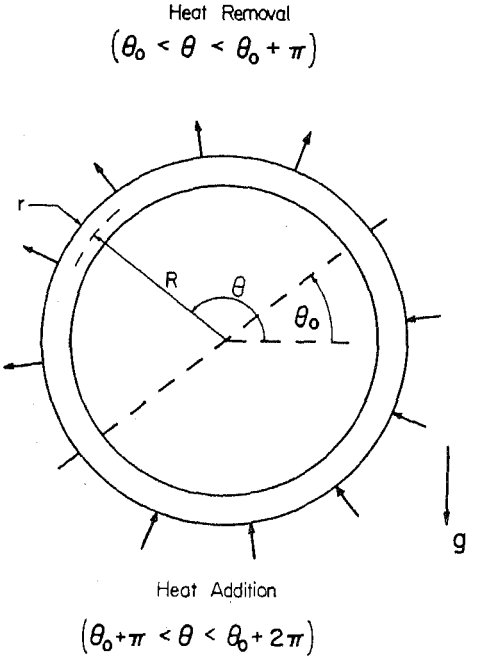

Fig. 1 Toroidal thermosyphon considered in the analysis

[1] This research was conducted while the first author was an NSF Graduate Fellow at Purdue University. Further details concerning this work are contained in an M.S.M.E. thesis [1].

Contributed by the Heat Transfer Division and presented at the AIAA/ASME Thermophysics and Heat Transfer Conference, Palo Alto, Calif., May 24–26, 1978. Manuscript received by the Heat Transfer Division July 28, 1979. Paper No. 78-HT-44.

mental control volume approach which assumes flow to be in the direction of increasing θ, the θ-direction momentum equation is written as

$$\tau_w(2\pi rR)d\theta + \rho g \cos\theta(\pi r^2 R)d\theta + \frac{dP}{d\theta}(\pi r^2)d\theta = 0 \quad (1)$$

which represents a balance of shear, body and pressure forces. When equation (1) is integrated from 0 to 2π, the integral of the pressure force term vanishes because pressure is a continuous function of θ. In integral form, equation (1) appears as

$$\frac{2}{rg}\int_0^{2\pi} \tau_w d\theta = -\int_0^{2\pi} \rho \cos\theta d\theta \quad (2)$$

Under the assumptions stated above, equation (2) is rewritten as

$$\frac{\pi f V^2}{2rg\beta} = \int_0^{2\pi} T\cos\theta d\theta \quad (3)$$

where T is the mixed mean temperature at a particular cross-section, V is the average fluid velocity, and the definition $\tau_w = f\rho V^2/8$ has been utilized. To solve equation (3) for V, the variation of T with respect to θ must be determined. This relationship is found from the energy equation, which is written as

$$\frac{dT}{d\theta} = \frac{2q_L''(\theta)R}{\rho_0 VrC} \quad (4)$$

where $q_L''(\theta)$ is the local wall heat flux at a given θ location. It is helpful at this point to consider two special cases for the function $q_L''(\theta)$.

1 $q_L''(\theta) = q''$ = constant (constant wall flux heat addition or heat removal).

2 $q_L''(\theta) = h(T_w - T)$, where the heat transfer coefficient h and the wall temperature T_w are both considered constant.

For case 1 (constant wall flux) the temperature distribution obtained from the energy equation is a linear function of θ. For case 2 the temperature distribution is exponential with respect to θ when h and T_w are constant.

Two different toroidal thermosyphons are now considered. In the first one, constant flux heat addition occurs over one-half the torus ($\theta_0 + \pi < \theta < \theta_0 + 2\pi$), and constant flux heat removal occurs over the remaining half ($\theta_0 < \theta < \theta_0 + \pi$). In the second thermosyphon, constant flux heat addition occurs over one-half the torus ($\theta_0 + \pi < \theta < \theta_0 + 2\pi$), and constant wall temperature heat removal occurs over the remaining half ($\theta_0 < \theta < \theta_0 + \pi$). It will be shown that the simpler analysis of the first thermosyphon (which is not physically practical) is under many conditions an accurate approximation to the second thermosyphon (which is physically practical).

Thermosyphon with Constant Flux Heating and Cooling. In this analysis $q_L''(\theta) = q''$ for $\theta_0 + \pi < \theta < \theta_0 + 2\pi$, and $q_L''(\theta) = -q''$ for $\theta_0 < \theta < \theta_0 + \pi$. By substituting these expressions into the energy equation, a solution for the temperature distribution is obtained. Utilizing continuity boundary conditions, the result is

$$T(\theta) = T(\theta_0) - \frac{2q''R}{\rho_0 VrC}(\theta - \theta_0) \quad (\theta_0 < \theta < \theta_0 + \pi) \quad (5)$$

$$T(\theta) = T(\theta_0) - \frac{2q''R}{\rho_0 VrC}(2\pi + \theta_0 - \theta) \quad (\theta_0 + \pi < \theta < \theta_0 + 2\pi) \quad (6)$$

Insertion of equations (5) and (6) into equation (3) and simplifying leads to

$$V^3 = \frac{16q''g\beta R}{\rho_0 Cf\pi}\cos\theta_0 \quad (7)$$

Based on laminar flow, $f = 64/\mathrm{Re}$, and equation (7) becomes

$$V^* = (\cos\theta_0)^{1/2} \quad (8)$$

where $V^* = V(2\pi\mu C/q''g\beta Rr)^{1/2}$, a dimensionless flow velocity.

The result expressed in equation (8) is shown graphically in Fig. 2. In the derivation of the momentum and energy equations it was assumed that flow was in the direction of increasing θ. Therefore, positive values of V^* represent counterclockwise flow and negative values represent clockwise flow. For a given θ_0, there are two analytically predicted steady flow velocities; they are equal in magnitude but one is in the counterclockwise direction and the other is in the clockwise direction.

Thermosyphon with Constant Flux Heating and Constant Wall Temperature Cooling. In this analysis $q_L''(\theta) = q''$ for $\theta_0 + \pi < \theta < \theta_0 + 2\pi$ and $q_L''(\theta) = h(T_w - T)$ for $\theta_0 < \theta < \theta_0 + \pi$, where h and T_w are considered constant. Using a procedure similar to the analysis shown above, it may be shown that

$$V^3 = (16q''g\beta R/f\rho_0 C\pi)[\cos\theta_0 + (hR/\rho_0 VrC)\sin\theta_0] \quad (9)$$

Based on the assumption of fully developed laminar flow, the expressions $f = 64/\mathrm{Re}$ and $h = 1.83k/r$ are substituted into equation (9). Although it was expected that the average value of h would be greater due to entrance effects, the fully developed value was adequate since the flow rate was found to be somewhat insensitive to moderate variations in the value of h. When these substitutions are made, equation (9) becomes

$$V^3 = (q''g\beta Rr/2\pi\mu C)[V\cos\theta_0 + (1.83kR/\rho_0 r^2 C)\sin\theta_0] \quad (10)$$

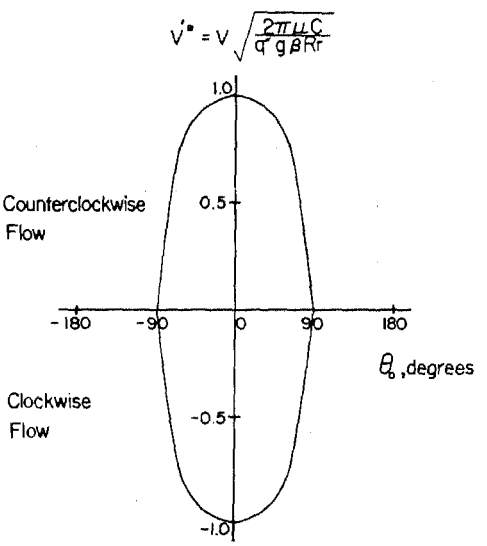

Fig. 2 Flow velocity for a thermosyphon with constant flux heating and cooling

Nomenclature

B = dimensionless quantity, equation (11)
C = specific heat
f = friction factor (Darcy)
g = acceleration due to gravity
h = heat transfer coefficient
k = thermal conductivity
$\dot{m}$ = mass flow rate
P = pressure
q'' = heat flux (constant)
q_L'' = local heat flux
R = major radius of torus
r = minor radius of torus
Re = Reynolds number
T = temperature
T_w = wall temperature
V = flow velocity
V^* = dimensionless flow velocity
α = arbitrary angle
β = thermal expansion coefficient
μ = dynamic viscosity
ρ = density
ρ_0 = density at reference temperature
θ = angular coordinate
θ_0 = angular displacement of heated and cooled sections
τ_w = wall shear stress

which can also be written as

$$(V^*)^3 - (V^*).\cos\theta_0 - (B)\sin\theta_0 = 0 \qquad (11)$$

where $V^* = V(2\pi\mu C/q''g\beta Rr)^{1/2}$ and

$$B = (1.83k/\rho_0 r^2)(2\pi\mu R/q''g\beta Cr)^{1/2} = \frac{hRr}{\rho_0(V/V^*)r^2C}$$

The second expression for B is seen to be a parameter indicating the number of transfer units (NTU) of the thermosyphon heat exchanger (i.e., NTU = (h) x (Area)/$(\dot{m})$ x (C)). According to equation (11), the variation of the dimensionless flow velocity V^* as a function of θ_0 will depend on the value of B, and hence will depend on the NTU of the thermosyphon. This dependence is shown in Fig. 3, where V^* is plotted versus θ_0 for several different values of B. These values of B are indicative of the range obtained in the experimental portion of this study.

By observing the thermosyphon from its back side, it is easily seen that clockwise flow for $\theta_0 = \alpha$ is physically identical to counterclockwise flow for $\theta_0 = -\alpha$, where α is any arbitrary angle. Thus, the curves in the first and third quadrants in Fig. 3 are identical, as are the curves in the second and fourth quadrants. The same statement applies to Fig. 2. In the neighborhood of maximum flow velocity between $\theta_0 = -60$ deg and +60 deg the curve given in Fig. 2 is essentially identical to that in Fig. 3. Hence, the constant flux model provides a simpler, though highly accurate, approximation to the thermosyphon with constant wall temperature cooling in this range. It is important to note that this conclusion applies only within the range of the values of B indicated in Fig. 3. As θ_0 is increased to 90 deg the curve of Fig. 2 approaches zero velocity, whereas the curves in Fig. 3 do not reach the axis until $\theta_0 = 180$ deg. Experimental observations confirmed that steady flow does exist in the range from $\theta_0 = 90$ to 180 deg. It is clear that the simpler constant flux model cannot be used as an approximation for operating conditions in this range. The reason that flows cannot exist beyond 90 deg in Fig. 2 is that the constant flux assumption results in a linear temperature distribution for which no solutions to equation (3) can be obtained when $\theta_0 > 90$ deg. This restriction to a linear temperature distribution is obviously not physically realistic for the low flows observed between 90 and 180 deg. However, the nonlinear temperature distribution permitted by the constant wall temperature assumption results in predicted flows in the region from 90 to 180 deg (Fig. 3). Moreover, the agreement between the two models for θ_0 less than 60 deg indicates that in this range the linear temperature distribution accurately approximates the temperature distribution in the constant wall temperature section.

The analysis performed here is only for the particular case in which the loop is heated over one half and cooled over the other half. However, the same technique could readily be used to analyze other heating and cooling distributions if analytical predictions for these cases are desired.

Experimental Apparatus

A schematic diagram of the experimental apparatus is shown in Fig. 4. The thermosyphon was fabricated from a Pyrex glass torus with a major radius of 0.38 m and a minor radius of 0.015 m. It was filled with distilled water. Heating elements were wound evenly around one-half of the torus, a close approximation to constant wall heat flux. Power was supplied to the heater through a variable transformer. A wattmeter in the heater circuit measured the power input to the system. Power input values ranged from zero to 1500 watts for the experiments, which corresponded to a heat flux range of zero to 13,300 watts/m^2. The heated portion of the torus was wrapped on the outside with insulation to minimize heat losses.

Heat was removed by an annular cooling jacket which surrounded the remaining half of the torus. Filtered tap water was used as the coolant. The tap water flow rate was metered, and temperatures at both the inlet and outlet of the cooling jacket were measured. From these measurements, it was possible to compare the input power with the energy removed by the coolant and thereby obtain an estimate

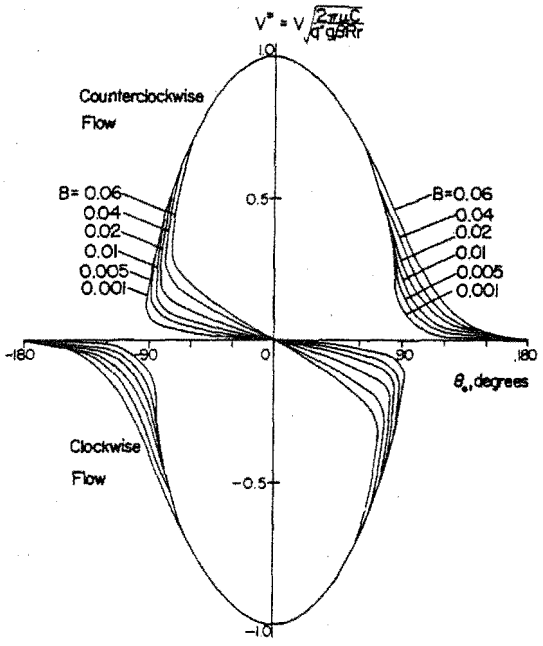

Fig. 3 Flow velocity for a thermosyphon with constant flux heating and constant wall temperature cooling

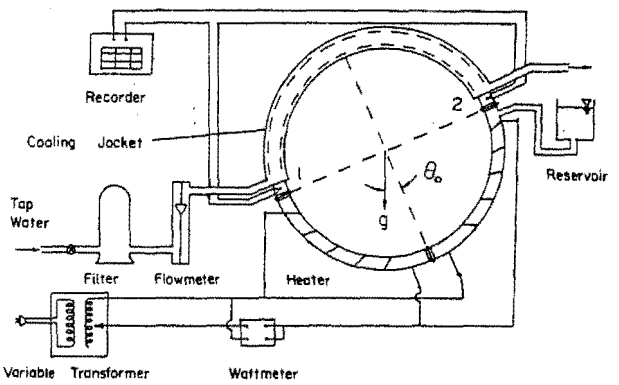

Fig. 4 Schematic diagram of experimental apparatus

of the energy losses from the system. In the majority of the test runs these losses were a small percentage of the input heating rate, usually less than 10 percent. Since the temperature of the tap water was very close to ambient room temperature, insulation around the cooling jacket was not required. This arrangement also allowed visualization of the flow in the cooled section.

By insuring that the flow rate of cooling water was much greater than the flow rate of the water inside the thermosyphon, a close approximation to constant wall temperature cooling was provided. Under these conditions the temperature change experienced by the coolant in passing through the jacket (usually much less than 1°C) was much smaller than the temperature change experienced by the internal fluid as it passed through this section (usually several degrees Celsius).

Two Chromel-Alumel thermocouples were installed inside the thermosyphon to measure the temperature difference between the locations just upstream and downstream of the heated section. With this measured temperature difference, the measured power input and the known specific heat of the internal fluid, the flow rate for the thermosyphon was calculated from an energy balance for each test run in which the flow was steady. When the flow was not steady, the sign of the temperature difference indicated the flow direction, as confirmed by visual observation.

Measurements of heat input and temperature difference were made with precision instruments and were believed to be adequately accurate (within ±5 percent). The greatest possible source of error in the calculation of flow rate was the assumption that the measured

temperature difference represented the actual difference in mixed mean temperature between the two points in the flow. An exact determination of the magnitude of this error was not performed. However, this error was believed to be minimized by placing the thermocouples at a radial location corresponding to the location of the mixed mean temperature for a fully developed laminar profile.

To provide angular displacement of the heated and cooled sections, the entire apparatus was mounted on a pivot at the center of the torus which allowed rotation in the vertical plane. Angular displacement was measured by suspending a plumb bob and measuring the angle between the plumb line and a fixed line on the apparatus. The reference geometry (zero displacement) was the configuration in which heating occurred from directly below and cooling from directly above.

Observed Flow Behavior

For each experiment the heat input, cooling water flow rate and angular displacement of the heated and cooled sections were adjusted to prescribed values. The system was then allowed to operate under these fixed conditions for a sufficient time period to allow transient effects to die out. In some cases a steady flow would then be established. In other instances, though, the flow would not achieve a steady value but would oscillate indefinitely. These oscillations continually amplified until the flow eventually reversed direction, whereupon amplifying oscillations occurred in the new flow direction. This behavior was not unexpected. Unstable flow in a toroidal thermosyphon had been previously observed and described by Creveling, et al. [5]. However, these previous observations had been made only for a thermosyphon heated from directly below and cooled from directly above, and the extent of this behavior when the heat addition and heat removal sections are displaced from this geometry was not known. Therefore, an experimental study of the stability behavior under the displaced condition ($\theta_0 \neq 0$) was performed as a part of the present investigation. The results are shown in Fig. 5, which contains a map of the experimentally observed stability behavior as a function of the input heat flux, q'', and the displacement angle of the heat transfer sections, θ_0. Two distinct regions of behavior are identified. For operating points located in the central enclosed region in Fig. 5, the flow oscillated indefinitely and never achieved a steady value. This region extended between values of θ_0 of -6 and $+6$ deg. For each value of θ_0 in this range there was an associated range of input heat flux for which unstable flow was observed.

For operating points outside the unstable flow region identified in Fig. 5, steady flow was observed when sufficient time was allowed for transient effects to die out. Except for the case of $\theta_0 = 0$, each stable condition yielded steady flow in one direction only. For each case in which θ_0 was greater than zero, the resulting steady flow was observed to occur in the counterclockwise direction. Similarly, for each case in which θ_0 was less than zero, the resulting steady flow was observed to occur in the clockwise direction. On an intuitive basis this behavior is not surprising. Even though flow in the opposite direction is somewhat plausible in light of the analysis just presented, steady flow in that direction was not observed. On the other hand, for θ_0 equal to zero, it was observed that the resulting steady flow could occur in either direction.

Comparison of Steady Flow Results with Analytical Predictions

As explained in the previous section, counterclockwise steady flow was found to be physically unachievable for $\theta_0 < 0$, and similarly clockwise steady flow was found to be physically unachievable for $\theta_0 > 0$. Therefore, experimental confirmation of the analytically predicted steady flow behavior in the second and fourth quadrants of Fig. 3 was not possible. Also, since the behavior in quadrant 3 is identical to that in quadrant 1, as previously discussed, it is only necessary to consider the first quadrant in comparing the observed and predicted flow velocities.

Fig. 6 shows a comparison of the experimentally observed steady flow velocities with the analytically predicted values in the first quadrant. Note that the analytically predicted results are represented

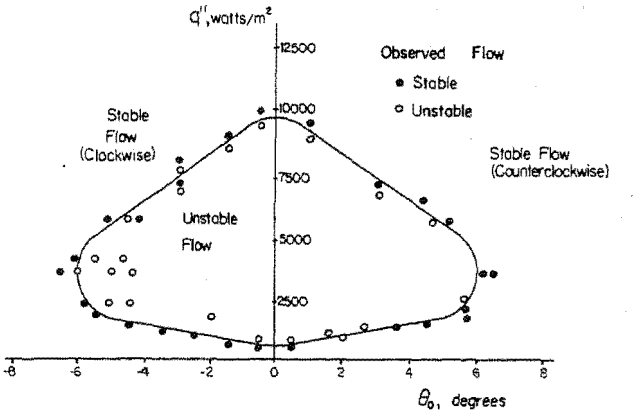

Fig. 5 Stability behavior of the experimentally observed flow

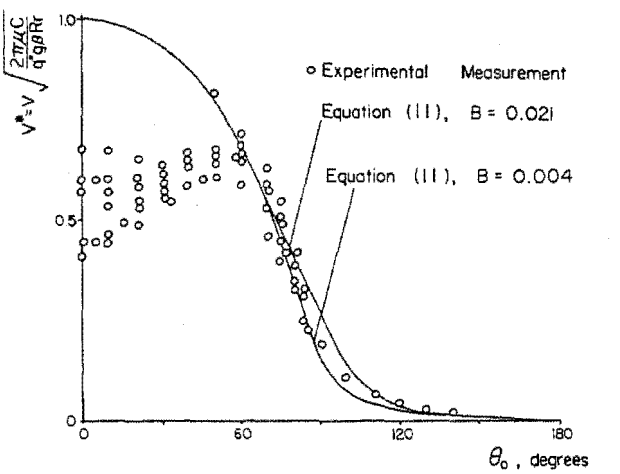

Fig. 6 Comparison of observed and predicted flow velocities

by two curves. Both curves correspond to equation (11), which was derived assuming laminar flow, but one curve is for a value of B equal to 0.004 and the other is for a value of B equal to 0.021. These are the minimum and maximum values of B calculated for the experiments. Hence, the two curves define a narrow envelope in which the experimental data should ideally lie. For $\theta_0 < 60$ deg and for $\theta_0 > 140$ deg the curves essentially coincide.

Trends in the experimental results are similar to analytical predictions, but the values of observed flow velocity are less than the corresponding analytically predicted values in the range of θ_0 between 0 and 60 deg. Between 60 and 140 deg the agreement between experiment and analysis is quite favorable. Experimental results were not obtainable for θ_0 greater than 140 deg because of potential overheating damage to the glass thermosyphon as a result of the very low flow rates in this range.

The experimentally measured values plotted in Fig. 6 cover a range of Reynolds number from 100 to 4000. Although this range nominally indicates cases of both laminar and turbulent flow, it was found that the data were most simply and effectively reduced when the laminar correlation for friction factor was used. (Recall that the dimensionless quantity V^* was derived employing the friction factor for fully developed laminar flow in a tube.) When a turbulent flow friction factor was used for those data points with Re values exceeding 2300, slight improvement in the comparison could be obtained, but considerable scatter of those points was observed. Therefore, it was deemed appropriate to plot all the data for the complete range of Re in a single representation for comparison with a single analytical model (Fig. 6).

One observation which seemed to explain the discrepancy between observed and predicted values of flow velocity was the presence of velocity profiles with reverse flow features in certain sections of the thermosyphon. These features were noted by inserting very small

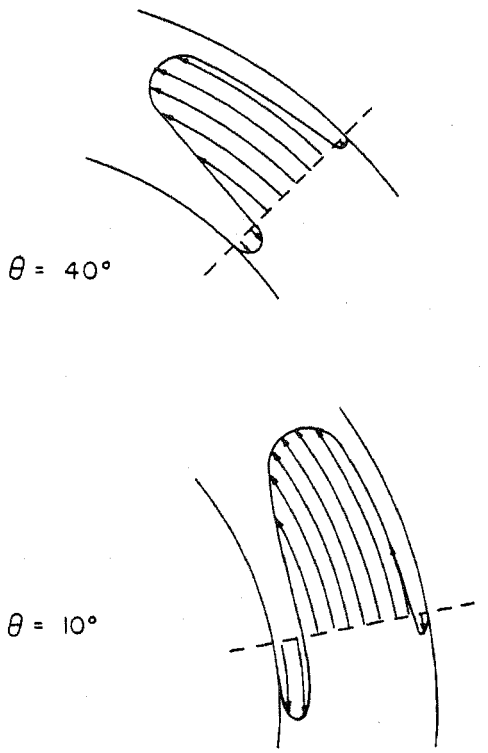

Fig. 7 Qualitatively observed velocity profiles with $\theta_0 = 0$ deg

plastic beads in the fluid and observing the flow patterns in the transparent cooled section. Fig. 7 shows two examples of the flow patterns observed in the thermosyphon. These profiles are qualitative representations based on visual observation only. Fig. 7 shows estimated profiles at the locations $\theta = 40$ deg and $\theta = 10$ deg, with θ_0 equal to zero (heating from directly below and cooling from directly above). Profiles of this type were observed over the range of θ-values from 0 to 60 deg. The reverse flow feature of this profile is apparently due to rapid cooling of the fluid near the wall of the torus. It is reasonable to expect that frictional losses associated with flow patterns like the ones shown in Fig. 7 would be greater than for fully developed laminar flow in a tube at a given Reynolds number. Thus, it is highly plausible that the presence of such flow patterns accounts for the observed velocities being somewhat lower than the corresponding predicted values. It was also observed that the magnitude of the reverse flows was greatest when θ_0 was equal to zero. Angular displacement of the heated and cooled sections from this geometry resulted in a diminishing of intensity of the reverse flow features, and a reduction of the range of θ-values in which these patterns were observed. For $\theta_0 > 60$ deg, reverse flow was not observed at all. This trend in the reverse flow parallels the discrepancy between the observed and predicted flow velocities shown in Fig. 6. It can be seen that the discrepancy between observed and predicted flow velocity is a maximum at θ_0 equal to zero, when reverse flow effects were greatest. The discrepancy diminishes as θ_0 approaches 60 deg, as did the observed reverse flow phenomena. For $\theta_0 > 60$ deg, where reverse flow was not observed, there is close agreement between observed and predicted flow velocities.

The observation of similar velocity profiles and overprediction of observed flow rates has also been noted by previous investigators. Hamilton, et al. [2] report both of these findings for flow in a thermal convection "harp," which consisted of a glass tube formed into a parallelogram with heating along one vertical leg and cooling along the other. Davies, et al. [3] report that the friction factor for flow in a rotating thermosyphon was significantly greater than for conventional flow in a tube. Creveling, et al. [5] also report similar reverse flow phenomena in a toroidal thermosyphon heated from below, and over-prediction of observed flow rates when standard correlations for friction factor were used. On the other hand, Lapin [8] conducted research using a rectangular thermosyphon heated along its bottom half and cooled along its upper half, but did not mention any observation of reverse flow. Also, it was reported that standard friction factor correlations for flow in a tube gave reasonably accurate predictions of the flow rate for this system. This result would not be expected based on the results of the present study.

Summary

1 The analysis predicts maximum flow rate in a toroidal thermosyphon when heating occurs from directly below and cooling from directly above (Figs. 2 and 3). This result is contrary to the suggestions of several previous reports in the literature.

2 Steady-state flow rate predictions based on the standard friction factor correlation for fully developed laminar flow exceed the corresponding experimentally observed values when the displacement angle of the heat transfer sections is between 0 and 60 deg (Fig. 6). A reverse flow phenomenon, as evidenced by visual observation, is apparently responsible for the overprediction of observed flow rates (Fig. 7). This effect was observed to be strongest when θ_0 was equal to zero, and was observed to subside to negligible significance as θ_0 approached 60 deg.

3 Steady-state flow rate predictions based on the standard friction factor correlation for fully developed laminar flow were found to be reasonably accurate when the displacement angle of the heat transfer sections was between 60 and 140 deg (Fig. 6).

4 Some analytically predicted steady flows were not physically achievable, apparently corresponding to unstable states of the system.

(*a*) For some operating conditions steady flow was never achieved experimentally. In these cases the flow oscillated indefinitely (Fig. 5).

(*b*) For some operating conditions more than one steady flow velocity was analytically predicted (Fig. 3). However, only one of these flow conditions was found to be physically achievable, that condition corresponding to flow in the direction of displacement of the heat transfer sections (Fig. 5). Flow in the opposite direction, although analytically predicted, was not observed experimentally. With $\theta_0 = 0$, however, steady flow in either direction was observed to occur within the stable ranges of heat flux shown in Fig. 5.

Acknowledgments

Support of the National Science Foundation through a graduate fellowship is gratefully acknowledged.

References

1 Damerell, P. S., "Flow in a Toroidal Thermosyphon with Angular Displacement of the Heated and Cooled Sections," M.S.M.E. Thesis, Purdue University, 1977.

2 Hamilton, D. C., Lynch, F. E. and Palmer, L. D., "The Nature of the Flow of Ordinary Fluids in a Thermal Convection Harp," Oak Ridge National Laboratory, ORNL-1624, 1954.

3 Davies, T. H. and Morris, W. D., "Heat Transfer Characteristics of a Closed Loop Rotating Thermosyphon," *Proceedings of the International Heat Transfer Conference*, 3rd, Chicago, Vol. 2, 1966, pp. 172–181.

4 Japikse, D., "Advances in Thermosyphon Technology," *Advances in Heat Transfer*, Vol. 9, Academic Press, New York, 1973, pp. 1–111.

5 Creveling, H. F., dePaz, J. F., Baladi, J. Y., and Schoenhals, R. J., "Stability Characteristics of a Single-Phase Free Convection Loop," *Journal of Fluid Mechanics*, Vol. 67, Part I, 1975, pp. 65–84.

6 Keller, J. B., "Periodic Oscillations in a Model of Thermal Convection," *Journal of Fluid Mechanics*, Vol. 26, 1966, pp. 599–606.

7 Welander, P., "On the Oscillatory Instability of a Differentially Heated Fluid Loop," *Journal of Fluid Mechanics*, Vol. 29, Part I, 1967, pp. 17–30.

8 Lapin, Y. D., "Heat Transfer in Communicating Channels Under Conditions of Free Convection," *Thermal Engineering* (USSR), 16(9), 1969, pp. 94–97.

9 "Flow of Fluids through Valves, Fittings and Pipe," Technical Paper No. 410, Crane Co., Chicago, 1957.